Journal of Theoretical and Applied Information Technology
15th September 2016. Vol.91. No.1

ISSN: 1992-8645 www.jatit.org E-ISSN: 1817-3195

ADAPTIVE BACKSTEPPING CONTROL FOR WIND TURBINES WITH DOUBLY-FED INDUCTION GENERATOR UNDER UNKNOWN PARAMETERS

[1]MOHAMMED RACHIDI, [2]BADR BOUOULID IDRISSI
[1,2]Department of Electromechanical Engineering, Moulay Ismaïl University, Ecole Nationale Supérieure d'Arts et Métiers, BP 4024, Marjane II, Beni Hamed, 50000, Meknès, Morocco

E-mail: [1]morachidi@yahoo.fr, [2]ibadr.bououlid@ensam.umi.ac.ma

ABSTRACT

This paper deals with an adaptive, nonlinear controller for wind systems connected to a stable electrical grid and using a doubly-fed induction machine as a generator. The study focuses on the case wherein the aerodynamic torque model and winding resistances of the generator are unknown and will be updating in real time. Two objectives were fixed; the first one is speed control, which allows us to force the system to track the optimal torque-speed characteristic of the wind turbine to extract the maximum power, and the second deals with the control of the reactive power transmitted to the electrical grid. The mathematical development, both for the model of the global system and the control and update laws, is examined in detail. The control design is investigated using a backstepping technique, and the overall stability of the system is shown by employing the Lyapunov theory. The results of the simulation, which was built on Matlab-Simulink, confirm when compared with control without adaptation, the validity of this work and the robustness of our control in the presence of parametric fluctuations or uncertainty modeling.

Keywords: *Wind power generation, doubly-fed induction generator, unknown winding resistances, unknown aerodynamic torque, adaptive control, backstepping control, Lyapunov theory.*

1. INTRODUCTION

From all sources of electricity generation, that which has the wind as origin has presented the highest growth rate for more than 20 years, and this should continue in the future [1]. Thus, wind generation should be the greatest contribution to reducing the greenhouse effect in the coming years. The causes for this increase lie in the high political will to promote this sector and also in production costs, which are becoming increasingly competitive. The most used structure in this area, especially in high power, which is also the subject of this work, is shown in Figure 1[2-3]. It uses a doubly fed induction machine as a generator. In general, the stator is directly connected to the electrical grid, but the rotor is connected through two back-to-back power converts and an RL filter. The capacitor C is considered as a DC regulated voltage source for the converts. The rotor side converter (RSC) is usually used to control the active and reactive power transmitted from the stator to grid. However, the grid side converter (GSC) is used to regulate the DC voltage at a fixed value and, at the same time, control the reactive power transmitted the from the RL filter to the grid. The principal benefit of this configuration is the possibility of varying the rotor speed in a large range around the synchronous speed of about ±30% [2-4]. This allows us to design a speed control that forces the system to continuously track the optimal torque-speed characteristic of the wind turbine [11-12].

The purpose of this work is to take part of this research area by examining the subject of the robustness of the control in case of parametric and modeling uncertainties. Indeed, we have targeted the pertinent parameters that are susceptible to vary with the temperature, such as the resistance of the rotor and stator windings. We also investigated the case of the aerodynamic torque, for which accurate modeling is not an easy task. We designed adaptive controllers that allow us to reach the fixed performances and, at the same time, to update the previous parameters that are assumed to be

Journal of Theoretical and Applied Information Technology
15th September 2016. Vol.91. No.1

ISSN: 1992-8645 www.jatit.org E-ISSN: 1817-3195

unknown. To show the importance of this study, we compared the performances of our control with those of the control without adaptation.

The paper is organized as follows. The second section presents a state-space modeling of the DFIG-based wind power conversion system. The third section details the proposed nonlinear adaptive controller. This design was established using backstepping technique and the Lyapunov approach. In the last section, we present the simulation results and discuss the importance of our study.

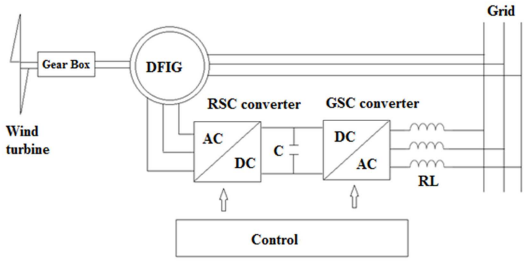

Figure. 1: DFIG-based wind power conversion system

2. SYSTEM MODEL

2.1. Modelling of the Wind Turbine

The aerodynamic turbine power P_t depends on the power coefficient Cp as follows [5]:

$$P_t = \frac{1}{2}\rho\,\pi\,R_t^2\,C_p(\lambda,\beta)\,v^3 \qquad (1a)$$

Where ρ, v, R_t, Cp, β, Ω et λ are the specific mass of the air, the wind speed, the radius of the turbine, the power coefficient, the blade pitch angle, the generator speed and the Tip Speed Ratio (TSR), respectively.

The TSR is given by: $$\lambda = \frac{R_t\,\Omega}{G\,v} \qquad (1b)$$

Where: G is the speed multiplier ratio.

The following equation is used to express Cp(λ,β) [5] as:

$$C_p(\lambda,\beta) = c_1\left(\frac{c_2}{\lambda_i} - c_3\beta - c_4\right)\exp\left(-\frac{c_5}{\lambda_i}\right) + c_6\lambda \qquad (1c)$$

Where $\frac{1}{\lambda_i} = \frac{1}{\lambda + 0.08\beta} - \frac{0.035}{\beta^3 + 1}$ and c_1 to c_6 are constants coefficients given in "Appendix". The power coefficient reaches its maximum (c_{pmax}) for β = 0° and a particular value λ_{opt} of λ. In this paper, we suppose that the wind turbine operates with β=0. To extract the maximum power and hence keep the TSR at λ_{opt} (MPPT strategy), a speed control must be done. According to (1b), the optimal mechanical speed is:

$$\Omega_c = \frac{G\,v}{R_t\,\lambda_{opt}} \qquad (1d)$$

2.2. Induction Generator Model

To get the model of the induction machine, we have applied the Park transformation in the synchronously rotating frame, with the d-axis is oriented along the stator-voltage vector position (v_{sd}=V, v_{sq}=0). In this reference frame, the electromechanical equations are [6]:

$$[V] = [R][I] + \frac{d[\phi]}{dt} + [\omega][\phi] \qquad (2a)$$

$$[\phi] = [M][I] \qquad (2b)$$

$$J\frac{d\Omega}{dt} = T_t - T_{em} - f\Omega \qquad (2c)$$

$$T_{em} = pL_m(i_{sq}i_{rd} - i_{sd}i_{rq}) \qquad (2d)$$

Where

$$[R] = \begin{bmatrix} Rs & 0 & 0 & 0 \\ 0 & Rs & 0 & 0 \\ 0 & 0 & Rr & 0 \\ 0 & 0 & 0 & Rr \end{bmatrix};$$

$$[M] = \begin{bmatrix} Ls & 0 & L_m & 0 \\ 0 & Ls & 0 & L_m \\ L_m & 0 & Lr & 0 \\ 0 & L_m & 0 & Lr \end{bmatrix};$$

$$[\omega] = \begin{bmatrix} 0 & -\omega_s & 0 & 0 \\ \omega_s & 0 & 0 & 0 \\ 0 & 0 & 0 & -\omega_r \\ 0 & 0 & \omega_r & 0 \end{bmatrix}$$

[V], [I] and [Φ] are the voltage, the current and the flux vectors. The subscripts s, r, d and q stand for stator, rotor, direct and quadratic, respectively.

R, L, L_m, ω, J, f, p, T_t and T_{em} are resistance, inductance, mutual inductance, electrical speed, total inertia, damping coefficient, number of pole pairs, mechanical torque and electromagnetic torque, respectively.

By choosing currents and speed as state variables, the system (2) can be put into the following state-space form:

$$\dot{x}_1 = g_1(x,R_r,R_s) + \beta u_1 \qquad (3a)$$

$$\dot{x}_2 = g_2(x,R_r,R_s) + \beta u_2 \qquad (3b)$$

$$\dot{x}_3 = g_3(x,R_r,R_s) + \alpha u_1 \qquad (3c)$$

$$\dot{x}_4 = g_4(x,R_r,R_s) + \alpha u_2 \qquad (3d)$$

ISSN: 1992-8645 www.jatit.org E-ISSN: 1817-3195

$$\dot{\eta} = -F\eta + \Gamma_t + \Gamma_{em} \quad (3e)$$

Where:

$$x = (x_1, x_2, x_3, x_4)^t = (i_{sd}, i_{sq}, i_{rd}, i_{rq})^t, \eta = \Omega$$

$$\Gamma_{em} = \frac{-T_{em}}{J} = a(x_1x_4 - x_2x_3); \Gamma_t = \frac{T_t}{J}$$

$$u_1 = v_{rd}, u_2 = v_{rq}$$

$$\alpha = \frac{1}{\sigma L_r}, \beta = -\frac{L_m}{\sigma L_r L_s}$$

The functions $g_i(x, R_r, R_s)$ are:

$$g_1 = -a_1R_sx_1 + b_1x_2 + c_1R_rx_3 + m_1x_2\eta + n_1x_4\eta + \alpha u$$
$$g_2 = -b_1x_1 - a_1R_sx_2 + c_1R_rx_4 - m_1x_1\eta - n_1x_3\eta$$
$$g_3 = c_3R_sx_1 - a_3R_rx_3 + b_3x_4 - n_3x_2\eta - m_3x_4\eta + \beta u$$
$$g_4 = c_3R_sx_2 - b_3x_3 - a_3R_rx_4 + n_3x_1\eta + m_3x_3\eta$$

$$a = \frac{pL_m}{J},\ a_1 = \frac{1}{\sigma L_s}, b_1 = \omega_s = 2\pi f_r, c_1 = \frac{L_m}{\sigma L_s L_r},$$
$$m_1 = p\frac{1-\sigma}{\sigma}, n_1 = p\frac{L_m}{\sigma L_s}, \alpha_u = \frac{1}{\sigma L_s}V,$$
$$a_3 = \frac{1}{\sigma L_r}, b_3 = 2\pi f_r, c_3 = \frac{L_m}{\sigma L_s L_r}, m_3 = \frac{p}{\sigma}, n_3 = p\frac{L_m}{\sigma L_r},$$
$$\beta_u = \beta V; \quad \sigma = 1 - \frac{L_m^2}{L_s L_r}; F = \frac{f}{J}$$

f_r and V are respectively the constant frequency and magnitude of grid voltage.

Equations (3a) to (3.d) can be put into the following compact form:

$$\dot{x} = g(x, R_r, R_s) + Au \quad (3f)$$

Where

$$g = (g_1, g_2, g_3, g_4)^t, \quad u = (u_1, u_2)^t,$$
$$A = \begin{bmatrix} \beta & 0 & \alpha & 0 \\ 0 & \beta & 0 & \alpha \end{bmatrix}^t$$

3. CONTROL DESIGN

3.1. Control objectives

By examining the equation system (3), we can identify two degrees of freedom u_1 and u_2 that can be used to control the RSC converter. Thus, two control objectives were set; the first one is speed control, which allows us to force the system to extract the maximum power, while the second deals with the control of reactive power transmitted by the stator to the electrical grid. To achieve this goal, we used the Backstepping technique [7-8]. Indeed, the following expression of the stator reactive power

$$Q_{sg} = \mathrm{Im}(\underline{V}\underline{I}^*) = v_{sq}i_{sd} - v_{sd}i_{sq} = -V x_2 \quad (4)$$

shows that the current variable x_2 can be used to control the reactive power Q_{sg}. According to equation (3b), it is clear that the control variable u_2 can be designed so that the current variable x_2 tracks its reference. On the other hand, from the system (3), we can reconstruct the following subsystem that adapts well to control speed:

$$\begin{cases} \dot{\eta} = -F\eta + \Gamma_t + \Gamma_{em} \\ \dot{\Gamma}_{em} = \nabla h \,.g + a\,(\beta x_4 - \alpha x_2)\,u_1 + a\,(\alpha x_1 - \beta x_3)\,u_2 \end{cases} \quad (5)$$

Where

$$h(x) = \Gamma_{em} = a(x_1x_4 - x_2x_3)$$

and $\nabla h = \left(\frac{\partial h}{\partial x_1}, \frac{\partial h}{\partial x_2}, \frac{\partial h}{\partial x_3}, \frac{\partial h}{\partial x_4}\right)$

So, in the first equation, the variable Γ_{em} can be considered as a virtual control for the speed η. The second equation shows that the control variable u_1 can be designed so that Γ_{em} tracks its reference.

3.1.2. Control and update laws

For uncertain model to which the parameters are not known with sufficient accuracy, an appropriate choice of control and update laws must be done to still ensure the stability condition. In this study, it is assumed that the stator resistance, rotor resistance and mechanical torque R_s, R_r and T_t, respectively, are unknown and vary slowly with time. Their corresponding estimated terms are denoted $\hat{R}_s$, $\hat{R}_r$ and $\hat{\Gamma}_t$, respectively. We define also the error variables as:

$$\begin{aligned} z_0 &= x_2 - x_{2c} \\ z_1 &= \eta - \eta_c \\ z_2 &= \Gamma_{em} - \Gamma_{emc} \\ \tilde{R}_r &= R_r - \hat{R}_r \\ \tilde{R}_s &= R_s - \hat{R}_s \\ \tilde{\Gamma}_t &= \Gamma_t - \hat{\Gamma}_t \end{aligned} \quad (6)$$

Where x_{2c}, η_c and Γ_{emc} are the references of variables x_2, η and Γ_{em}, respectively.

Proposition: *The following update and control laws:*

ISSN: 1992-8645 www.jatit.org E-ISSN: 1817-3195

$$\begin{cases}\dot{\xi} = -\lambda_t\xi_t - \lambda_t h(x) + \lambda_t(F-\lambda_t)\eta - v_t \\ \hat{\Gamma}_t = \xi_t + \lambda_t\eta\end{cases}$$

$$\dot{\hat{R}}_r = \gamma_r(c_1 x_4 z_0 - a_3 h(x) z_2)$$

$$\dot{\hat{R}}_s = -\gamma_s a_1(x_2 z_0 + h(x) z_2)$$

$$u_2 = \frac{-g_2(x,\hat{R}_r,\hat{R}_s) - k_0 z_0 + \dot{x}_{2c}}{\beta};$$

$$u_1 = \frac{\hat{\upsilon} - \nabla h.\hat{g} - a(\alpha x_1 - \beta x_3)u_2}{a(\beta x_4 - \alpha x_2)}$$

With

$$\Gamma_{emc} = -(k_1 - F)z_1 + F\eta_c - \hat{\Gamma}_t + \dot{\eta}_C$$

$$\Gamma_{em} = h(x) = a(x_1 x_4 - x_2 x_3)$$

$$v_t = -z_1 - (\lambda_t + k_1 - F)z_2$$

$$\hat{\upsilon} = z_1 - k_2 z_2 + F\dot{\eta}_c + (k_1 - F)(k_1 z_1 + z_2) + \ddot{\eta}_C + v_t$$

$$\nabla h.\hat{g} = a(x_1 g_4(x,\hat{R}_r,\hat{R}_s) + x_4 g_1(x,\hat{R}_r,\hat{R}_s) - x_2 g_3(x,\hat{R}_r,\hat{R}_s) - x_3 g_2(x,\hat{R}_r,\hat{R}_s))$$

$k_0, k_1, k_2, \gamma_r, \lambda_t$ are positives design constants

achieve speed and current tracking objectives and ensure asymptotic stability despite the changes in parameters.

Proof:

a- Control law u_2

Taking the derivative of z_0 and using (3b), we can write:

$$\dot{z}_0 = g_2(x,R_r,R_s) + \beta u_2 - \dot{x}_{2c} \quad (7)$$

With the Lyapunov candidate function $V_0 = \frac{1}{2}z_0^2$ and the choice $\dot{z}_0 = -k_0 z_0$, where k_0 is a positive design constant, it's possible to make negative the derivative $\dot{V}_0 = -k_0 z_0^2 \le 0$.

The control law u_2 can be obtained from equation (7), using the previous choice and the estimated resistances, as:

$$u_2 = \frac{-g_2(x,\hat{R}_r,\hat{R}_s) - k_0 z_0 + \dot{x}_{2c}}{\beta} \quad (8)$$

So, the dynamic of the error z_0 is governed by:

$$\dot{z}_0 = -k_0 z_0 + c_1\tilde{R}_r x_4 - a_1\tilde{R}_s x_2 \quad (9)$$

This can be obtained from (7) by using (8) and noting that

$$g_2(x,R_r,R_s) = g_2(x,\hat{R}_r,\hat{R}_s) - a_1\tilde{R}_s x_2 + c_1\tilde{R}_r x_4.$$

b- Control u_1 and update laws

Step 1: Virtual control Γ_{emc}

Using equation (3e), the derivative of z_1 is written as:

$$\dot{z}_1 = -F\eta + \Gamma_t + \Gamma_{em} - \dot{\eta}_C \quad (10)$$

Since Γ_t is unknown; it will be replaced with its estimated $\hat{\Gamma}_t$. With the Lyapunov candidate function $V_1 = \frac{1}{2}z_1^2$ and the choice $\dot{z}_1 = -k_1 z_1$, where k_1 is a positive design constant, it's possible to make negative the derivative $\dot{V}_1 = -k_1 z_1^2 \le 0$.

Using this choice, equation (10) becomes:

$$-k_1 z_1 = -F\eta + \hat{\Gamma}_t + \Gamma_{emc} - \dot{\eta}_C \quad (11)$$

Thus, the virtual control Γ_{emc} is:

$$\Gamma_{emc} = -(k_1 - F)z_1 + F\eta_c - \hat{\Gamma}_t + \dot{\eta}_C \quad (12)$$

Where η has been replaced by $z_1 + \eta_c$

Subtracting (11) from (10), we obtain:

$$\dot{z}_1 = -k_1 z_1 - z_2 + \tilde{\Gamma}_t \quad (13)$$

Step 2: Control and update laws

We will now proceed in the same way for the derivative $\dot{z}_2$.

$$\dot{z}_2 = \dot{\Gamma}_{em} - \dot{\Gamma}_{emc} \quad (14)$$

Firstly, we express $\dot{\Gamma}_{em}$ according to (5):

Using (6), the detailed development of the term $\nabla h\,.g$ gives:

$$\nabla h\,.g = \nabla h.\hat{g} - a_3\tilde{R}_r h(x) - a_1\tilde{R}_s h(x)$$

Where

$$\nabla h.\hat{g} = a(x_1 g_4(x,\hat{R}_r,\hat{R}_s) + x_4 g_1(x,\hat{R}_r,\hat{R}_s) - x_2 g_3(x,\hat{R}_r,\hat{R}_s) - x_3 g_2(x,\hat{R}_r,\hat{R}_s))$$

To separate unknown terms from the rest, we write $\dot{\Gamma}_{em}$ as:

$$\dot{\Gamma}_{em} = \hat{\upsilon} - a_3\tilde{R}_r h(x) - a_1\tilde{R}_s h(x)$$

Where

$$\hat{\upsilon} = \nabla h.\hat{g} + a(\beta x_4 - \alpha x_2)u_1 + a(\alpha x_1 - \beta x_3)u_2 \quad (15)$$

Secondly, taking the derivative of Γ_{emc} from (12) and using (13), we can write $\dot{\Gamma}_{emc}$ as:

Journal of Theoretical and Applied Information Technology
15th September 2016. Vol.91. No.1

ISSN: 1992-8645 www.jatit.org E-ISSN: 1817-3195

$$\dot{\Gamma}_{emc} = -(k_1 - F)(-k_1 z_1 - z_2 + \tilde{\Gamma}_t) + F\dot{\eta}_c - \dot{\tilde{\Gamma}}_t + \ddot{\eta}_C$$

Thus the dynamic of error z_2 is:

$$\begin{aligned}\dot{z}_2 = \; & \hat{\upsilon} - a_3\tilde{R}_r h(x) - a_1\tilde{R}_s h(x) + (k_1 - F)(-k_1 z_1 \\ & - z_2 + \tilde{\Gamma}_t) - F\dot{\eta}_c + \dot{\tilde{\Gamma}}_t - \ddot{\eta}_C\end{aligned} \quad (16)$$

To update the torque, one proposes the dynamic of error estimation $\tilde{\Gamma}_t$ as [9]:

$$\dot{\tilde{\Gamma}}_t = -\lambda_t\tilde{\Gamma}_t + v_t \quad (17)$$

Where λ_t is a positive design constant and v_t is a term to be determined after.

If we combine (17) and the equation of motion (3e), we can establish the update law of the torque as:

$$\dot{\hat{\Gamma}}_t - \lambda_t\dot{\eta} = -\lambda_t(\hat{\Gamma}_t - \lambda_t\eta) - \lambda_t h(x) + \lambda_t(F - \lambda_t)\eta - v_t$$

For this law, we have assumed that the torque varies slowly, which results in: $\dot{\tilde{\Gamma}}_t = -\dot{\hat{\Gamma}}_t$

By using $\xi_t = \hat{\Gamma}_t - \lambda_t\eta$ as intermediate variable, one can rewrite the update law of the torque as:

$$\begin{cases}\dot{\xi}_t = -\lambda_t\xi - \lambda_t h(x) + \lambda_t(F - \lambda_t)\eta - v_t \\ \hat{\Gamma}_t = \xi_t + \lambda_t\eta\end{cases} \quad (18)$$

Equation (16) can be now put in the form:

$$\dot{z}_2 = \; A - a_3\tilde{R}_r h(x) - a_1\tilde{R}_s h(x) + (\lambda_t + k_1 - F)\tilde{\Gamma}_t \quad (19)$$

Where

$$A = \hat{\upsilon} - F\dot{\eta}_c + (k_1 - F)(-k_1 z_1 - z_2) - \ddot{\eta}_C - v_t \quad (20)$$

To ensure the overall stability, one proposes the following Lyapunov candidate function:

$$V = \frac{1}{2}z_0^2 + \frac{1}{2}z_1^2 + \frac{1}{2}z_2^2 + \frac{1}{2\gamma_r}\tilde{R}_r^2 + \frac{1}{2\gamma_s}\tilde{R}_s^2 + \frac{\tilde{\Gamma}_t^2}{2} \quad (21)$$

Using (9), (13) and (19), $\dot{V}$ can be written as follows:

$$\begin{aligned}\dot{V} = & -k_0 z_0^2 - k_1 z_1^2 + (A - z_1)z_2 - \lambda_t\tilde{\Gamma}_t^2 + (c_1 x_4 z_0 - a_3 h(x)z_2 \\ & - \frac{1}{\gamma_r}\dot{\tilde{R}}_r)\tilde{R}_r + (z_1 + (\lambda_t + k_1 - F)z_2 + v_t)\tilde{\Gamma}_t \\ & + (-a_1 x_2 z_0 - a_1 h(x)z_2 - \frac{1}{\gamma_s}\dot{\tilde{R}}_s)\tilde{R}_s\end{aligned}$$

The update laws are obtained by cancelling the terms with $\tilde{R}_r$ and $\tilde{\Gamma}_t$:

$$v_t = -z_1 - (\lambda_t + k_1 - F)z_2$$

$$\dot{\tilde{R}}_r = \gamma_r(c_1 x_4 z_0 - a_3 h(x)z_2)$$

$$\dot{\tilde{R}}_s = -\gamma_s a_1(x_2 z_0 + h(x)z_2)$$

By choosing $A = z_1 - k_2 z_2$, equation (19) becomes:

$$\dot{z}_2 = z_1 - k_2 z_2 - a_3\tilde{R}_r h(x) - a_1\tilde{R}_s h(x) - (\lambda_t + k_1 - F)\tilde{\Gamma}_t \quad (22)$$

And the derivative $\dot{V}$ reduces to:

$$\dot{V} = -k_0 z_0^2 - k_1 z_1^2 - k_2 z_2^2 - \lambda_t\tilde{\Gamma}_t^2 \le 0$$

Which implies that the errors z_0, z_1, z_2 and $\tilde{\Gamma}_t$ converge to zero.

Equations (9) and (22) show that if h(x) is different from zero then, errors $\tilde{R}_r$ and $\tilde{R}_s$ converge also to zero.

Finally, by using (15) one can establish the control law u_1 as:

$$u_1 = \frac{\hat{\upsilon} - \nabla h.\hat{g} - a(\alpha x_1 - \beta x_3)u_2}{a(\beta x_4 - \alpha x_2)}$$

For this expression, the term $\hat{\upsilon}$ is determined, by replacing the term A in the equation (20) by $z_1 - k_2 z_2$, as:

$$\hat{\upsilon} = z_1 - k_2 z_2 + F\dot{\eta}_c + (k_1 - F)(k_1 z_1 + z_2) + \ddot{\eta}_C + v_t$$

Remark:

$$a(\beta x_4 - \alpha x_2) = a(-\frac{1}{\sigma L_r}i_{sq} - \frac{L_m}{\sigma L_r L_r}i_{rq}) = -\frac{a}{\sigma L_r L_r}\phi_{sq}$$

Since the effect of the stator resistance is negligible especially in high power, the flux and the voltage vectors are substantially orthogonal. Then, with the frame used for the induction machine, the term $|\phi_{sq}|$ is equal to the amplitude of the stator flux. Consequently, the term $a(\beta x_4 - \alpha x_2)$ becomes different from zero as soon as the system is connected to the grid.

4. SIMULATION RESULTS

The simulation built on Matlab / Simulink deals with the entire wind system shown in Figure 1. In a previous paper [10], we developed the GSC converter control and for which we are interested for regulating the DC voltage and reactive power transmitted from the rotor to the grid. This power is proportional to the quadratic component of the phase current, noted i_{0q}, passing through the filter RL (see Eq(4)). To show the importance of this paper, we developed two simulation schemes, which corresponded respectively to the conventional (with known model) and our adaptive

ISSN: 1992-8645 www.jatit.org E-ISSN: 1817-3195

(with unknown resistances and mechanical torque model) backstepping controllers.

The tracking and identifying capability of our adaptive controller were verified in the case of time-varying wind speed (Figures 3). To demonstrate the robustness against winding resistances and mechanical torque changes, regulation performances for adaptive and conventional controllers were compared at constant wind speed (Figures 4). For both cases, one assumes that changes occur in the system model, first (at 10s, $\Delta Rr=50\%$) and next in the mechanical torque (at 20s, $\Delta T_t=-50\%$).

The constant values for DC-link voltage filter and quadratic currents references were considered. To have a unity power factor, the references of q-axis currents i_{sq} and i_{oq} have been set to zero. The values of the design parameters used in simulation are:

k_0 =1000, k_1 =150, k_2 =2000, λ_t=10 and $\gamma_s=\gamma_r$ =0.0001.

Figures 3a and 3b confirm the effectiveness of the MPPT strategy since the rotor speed varies in accordance with wind speed so that the turbine operates at its optimal TSR.

Figures 3d and 3e show the good tracking capability of the q-axis current controller. The same performances are achieved in the case of DC-link regulation (Figure 3f) and the virtual control variable (Figure 3c).

Figures 3g and 3h illustrate the two operating modes of the generator. Around time t=55s, we can see in Figure 3b that the induction machine switches from super-synchronous to sub-synchronous mode (Ns=1500 rpm). Figure 3g shows that grid voltage and stator current are in phase for both of the two operating modes; thus, the active power is transmitted from the stator to the grid. Figure 3h shows that grid voltage and filter current are in phase opposition for (t>55s); thus, the active power is transmitted from the grid to the rotor. This result is compatible with the sub-synchronous speed operation. Also, Figure (3h) shows that, for (t<55s), the grid voltage and filter current are in phase; thus, the active power is transmitted from the grid to the rotor. This result is compatible with the super-synchronous speed operation.

According to Figure 3i, one can notice that the unknown rotor resistance quickly converges to its true profile (unknown to the controller). Likewise, Figure 3j shows that the estimated mechanical torque recovers perfectly the applied unknown aerodynamic torque.

Figure 4 shows the regulation performances of the conventional and adaptive controllers when there are changes in the rotor resistance Rr and the mechanical torque Tt. The simulation assumes that changes occur in the system model first at 10s, $\Delta Rr=50\%$ and next in the mechanical torque at 20s, $\Delta Tt=-50\%$. Unlike the conventional backstepping controller (Figures. 4b, 4d, and 4f), the adaptive controller tracks correctly the references of regulated variables despite the changes (Figures. 4a, 4c, and 4e). These results confirm the robustness of the proposed controller.

5. CONCLUSION

This paper has shown the effectiveness and robustness of a nonlinear, adaptive, backstepping controller in variable-speed DFIG systems with unknown aerodynamic torque models and unknown resistances of rotor and stator winding. The numerical simulation shows the good speed, current tracking performances, and the correct update and identification of unknown parameters. Finally, the comparison with the conventional controller without adaptations shows the superiority of the proposed adaptive controller and the pertinence of this work.

ISSN: 1992-8645 www.jatit.org E-ISSN: 1817-3195

Appendix: Characteristics and Parameters

Induction Generator	
Rated power	3MW
Rated stator voltage	690V
Nominal frequency	50Hz
Number of pole pairs	p =2
Rotor resistance	R_s=2.97e-3Ω
Stator resistance	R_r=3.82e-3Ω
Stator inductance	L_s=0.0122H
Rotor inductance	L_r=0.0122H
Mutual inductance	L_m=12.12e-3H
Wind Turbine	
Blade Radius	R_t=45m
Power coefficient	C_{pmax}= 0.48
Optimal TSR	λ_{opt}=8.14
Mechanical speed multiplier	G=100
Cp coefficients	c_1 = 0.5176, c_2 = 116, c_3 = 0.4, c_4 = 5, c_5 = 21 c_6 = 0.0068
Generator and Turbine	
Moment of inertia	J=254Kg .m^2
Damping coefficient	F=0.24
Bus DC	C = 38 mF, v_{dc} = 1200 V
Filter RL	R = 0,075 Ω, L = 0,75 mH
Electrical grid	U = 690 V, f = 50 Hz

REFERENCES:

[1] B. Multon ; X. Roboam ; B Dakyo ; C. Nichita ; O Gergaud ; H. Ben Ahmed, "Aérogénérateurs électriques", techniques de l'Ingénieur, Traités de génie électrique, D3960, Novembre 2004.

[2] R. Pena, J. C. Clare, G. M. Asher, "Doubly fed induction generator using back-to-back PWM converters and its application to variable -speed wind-energy generation," IEE Proc. Electr. Power Appl., vol. 143, no. 3, pp. 231-241, May 996.

[3] Karthikeyan A., Kummara S.K, Nagamani C. and Saravana Ilango G, " Power control of grid connected Doubly Fed Induction Generator using Adaptive Back Stepping approach", in Proc 10th IEEE International Conference on Environment and Electrical Engineering EEEIC-2011, Rome, May 2011.

[4] H. Li, Z. Chen, "Overview of different wind generator systems and their comparisons" IET Renewable Power Generation, 2008, 2(2):123-138.

[5] Siegfried Heier, "Grid Integration of Wind Energy Conversion Systems" John Wiley & Sons Ltd, 1998, ISBN 0-471-97143-X.

[6] J.P.Caron, J.P.Hautier, 1995 "Modélisation et Commande de la Machine Asynchrone" Edition Technip, Paris.

[7] M. Krstic, I. Kanellakopoulos, P. Kokotovic, "Nonlinear and adaptive control design", John Wiley & Sons, Inc, 1995.

[8] I. Kanellakopoulos, P.V. Kokotovic, and A.S. Morse, "Systematic design of adaptive controller for feedback linearizable systems", IEEE Trans. Auto. Control. 1991. Vol. 36, (11), pp. 1241-1253.

[9] Marino, Riccardo, Tomei, Patrizio, Verrelli, Cristiano M. '' Induction Motor Control Design" Springer-Verlag London, 2010.

[10] M. Rachidi, B.Bououlid , "Adaptive Nonlinear Control of Doubly-Fed Induction Machine in Wind Power Generation" Journal of Theoretical and Applied Information Technology May 2016, Vol 87, N°1.

[11] E. Koutroulis and K. Kalaitzakis, "Design of a Maximum Power Tracking System for Wind-Energy-Conversion Applications" IEEE Transactions On Industrial Electronics, Vol. 53, No. 2, April 2006.

[12] Y.Hong, S. Lu, C. Chiou, "MPPT for PM wind generator using gradient approximation", Energy Conversion and Management 50 (1), pp. 82-89, 2009

Journal of Theoretical and Applied Information Technology
15th September 2016. Vol.91. No.1

ISSN: 1992-8645 www.jatit.org E-ISSN: 1817-3195

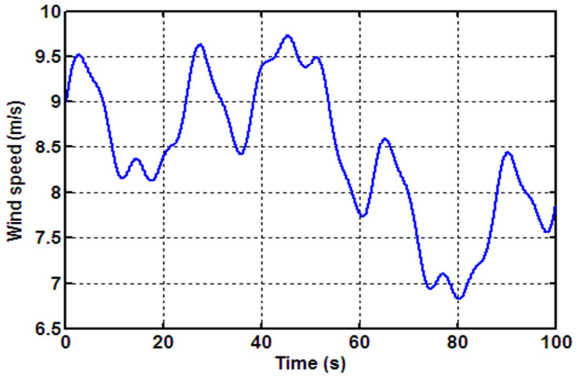

Fig. 3a: Time-varying wind speed

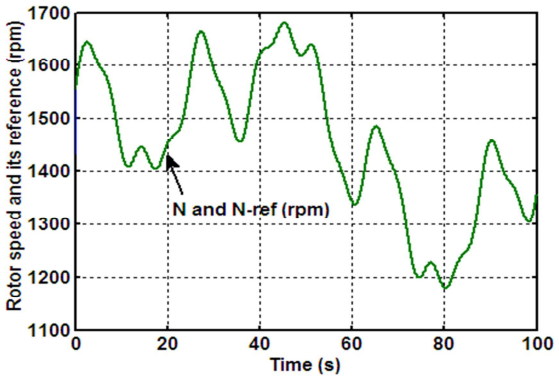

Fig. 3b: Rotor speed and its reference

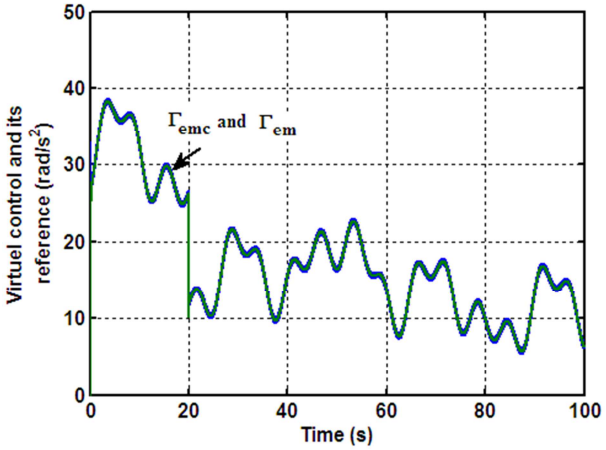

Fig. 3c: virtual control and its reference

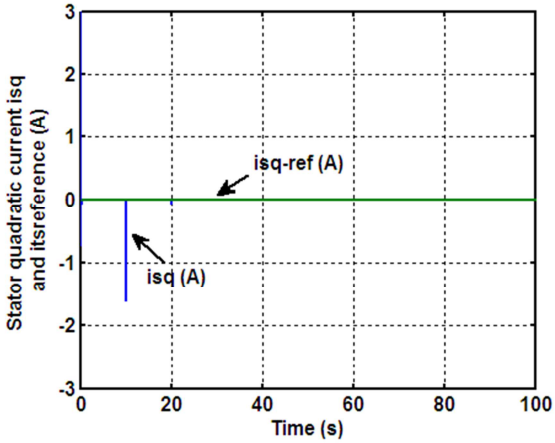

Fig. 3d: Stator q-axis current and its reference

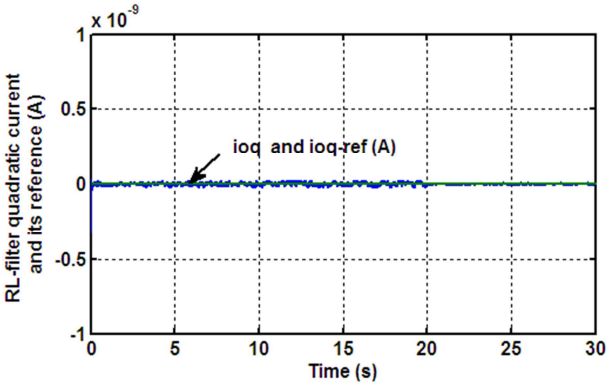

Fig. 3e: Filter q-axis current and its reference

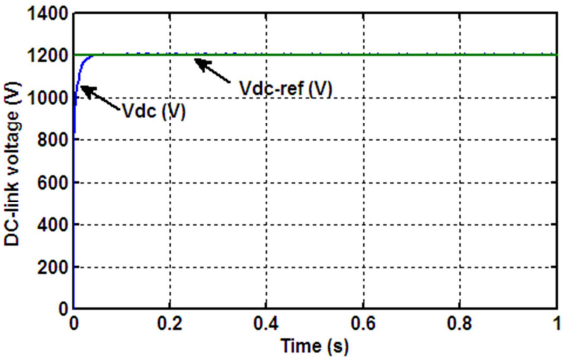

Fig. 3f: DC-link voltage and its reference

Journal of Theoretical and Applied Information Technology
15th September 2016. Vol.91. No.1

ISSN: 1992-8645 www.jatit.org E-ISSN: 1817-3195

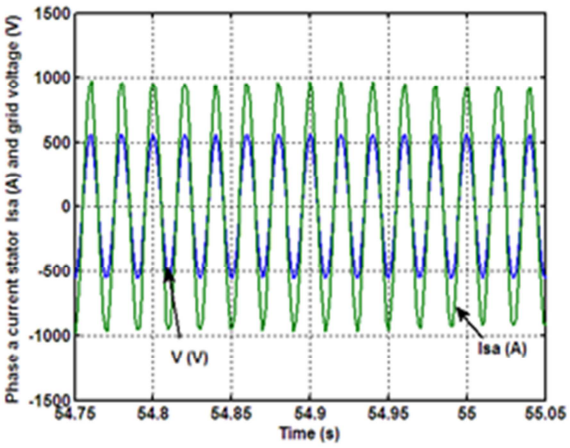

Fig. 3g: Phase a grid voltage and stator current

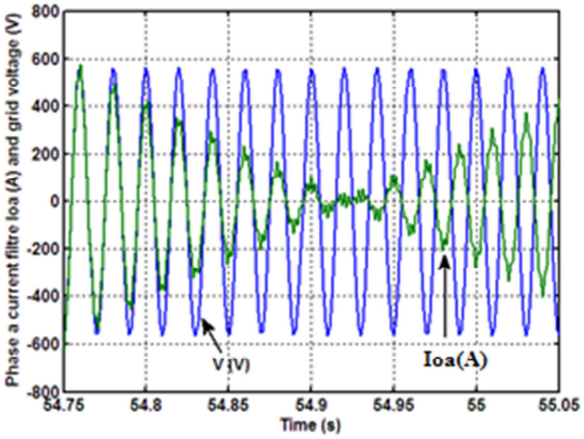

Fig. 3h: Phase a grid voltage and filter current

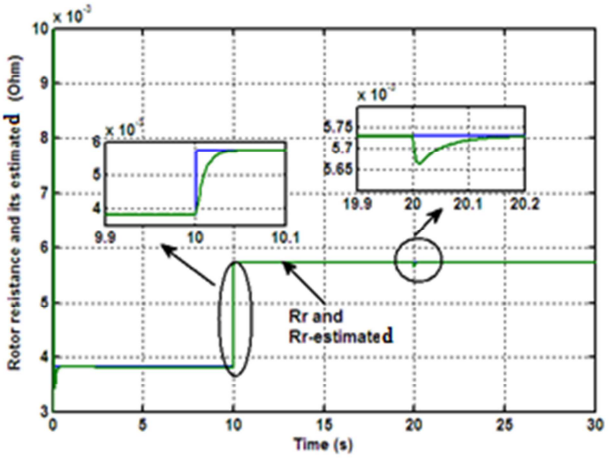

Fig. 3i: Rotor resistance and its estimated

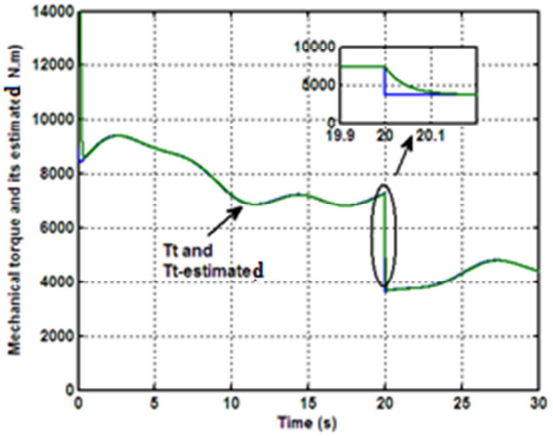

Fig. 3j: Mechanical torque and its estimated

Figure 3: Tracking capability under time-varying wind speed
Changes occur at 10s (ΔRr=50%) and at 20s (ΔT_t=-50%)

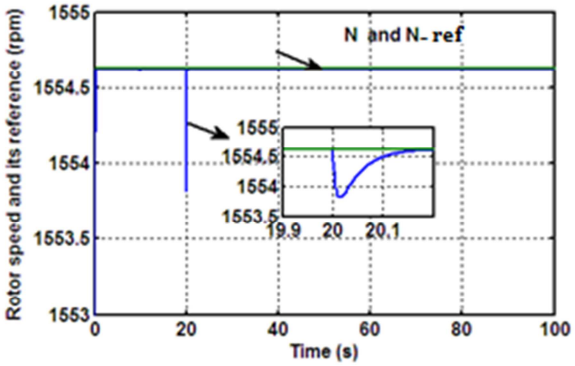

Fig. 4a: Rotor speed with adaptation

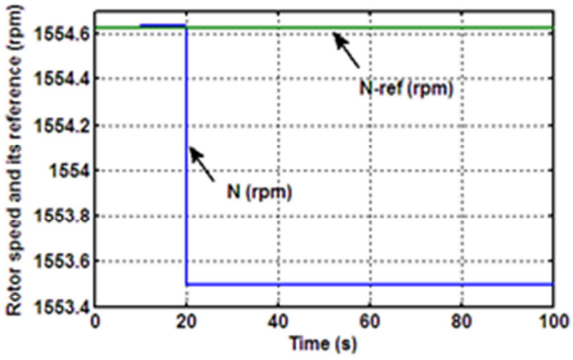

Fig. 4b: Rotor speed without adaptation

Journal of Theoretical and Applied Information Technology
15th September 2016. Vol.91. No.1

ISSN: 1992-8645 www.jatit.org E-ISSN: 1817-3195

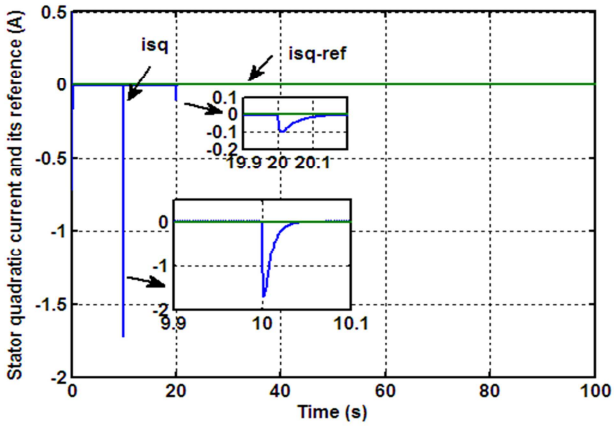

Fig. 4c: Stator current with adaptation

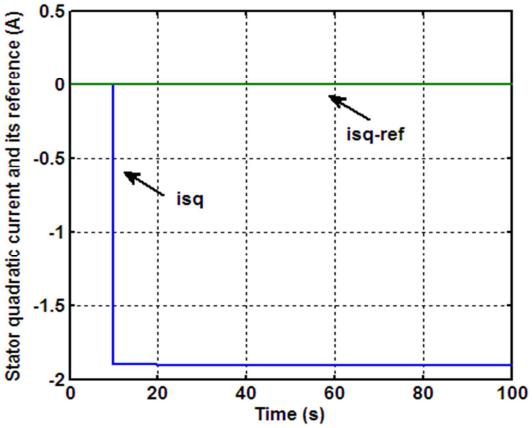

Fig. 4d: Stator current without adaptation

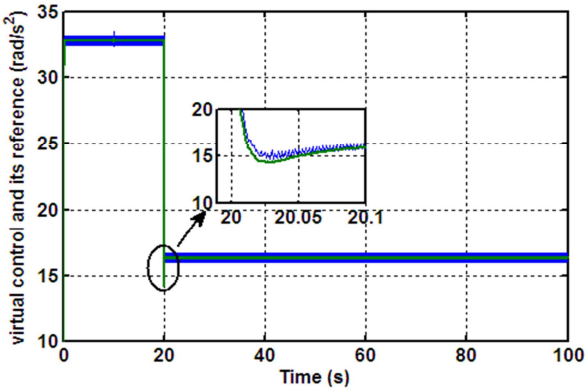

Fig. 4e: Virtual control with adaptation

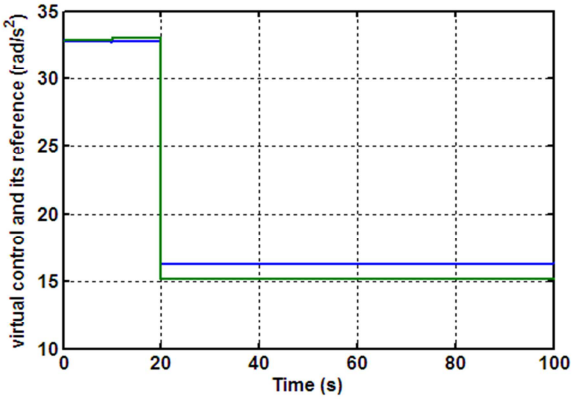

Fig. 4f: Virtual control without adaptation

Figure 4: Comparison of tracking performances under unknown parameters
Changes occur at 10s (ΔRr=50%) and at 20s (ΔT_t=-50%)